Large area HgI_2 polycrystalline films for X-Ray imager

G. XU[a], J. Y. LI[a], R. H. NAN[a], W. L. ZHOU[a], Z. GU[b], L. ZHANG[c], X. M. MA[c], X. P. CAO[c]

[a]*School of Materials and Chemical Engineering, Xi'an Technological University, Xi'an 710032, P.R.China;*

[b]*State Key Laboratory of Solidification Processing, North western Polytechnical University, Xi'an, 710072, P.R.China;*

[c]*Nuctech Company Limited, Beijing, 100084, P.R.China*

1 cm^2 and 36 cm^2 area of HgI_2 polycrystalline films were grown by physical vapor deposition (PVD), respectively. The properties of films with areas of 1 cm^2 were investigated by XRD, SEM and *J-V* analysis as prior period research. The results of XRD show that the ratio of (001) / (hkl) is amount to be 90%. Grain size of films grown was measured to be 120-150 μm, and their electrical resistivity were also determined as about 10^{11} Ω·cm operated at the bias voltage of ~100 V by *I-V* characteristic measurement. Larger one with 36 cm^2 areas was then deposited on TFT after craft optimization. The oriented of films were also measured by XRD, which show that the oriented of grains decrease with area. Image prepared after capsulation was tested for non-corrosive nut imaging. X-ray imager was made of 36 cm^2 HgI_2 polycrystalline films. A256×256 pixels X-ray image of a non-corrosive nut was obtained under 80KeV with 6mA. The outer hexagon and the inner circular shape of the nut are distinct, which shows that the films meet the need of dental X-ray unit.

(Received July 30, 2015; accepted September 29, 2016)

Keywords: Mercuric iodide, polycrystalline, X-ray imaging

1. Introduction

The development of direct-conversion flat-panel X-ray digital image detectors for medical diagnostic, scientific, and industrial applications has attracted significant attention during the past 15 years [1-5]. X-ray imaging of small animals is also increasing as animal models are used in disease and drug studies [6].Mercuric iodide, as a group of wide band gap semiconductors, has been widely investigated during most of the last half-century. However, the widespread deployment of this material for X-ray and gamma radiation detection has been held back by the high cost of single crystals grown by the slow physical vapor deposition[4], and impurities or/and defects, introduced by the growth process or by subsequent detector fabrication process, undoubtedly affecting the achievement of optimum detector properties. Barber reported that film with the thickness of 150μm was sufficient for 99% stopping up to 50keV[7]. Now, due to the low cost and ease of fabrication of large-area detectors, polycrystalline thin/thick films of mercuric iodide now have considerable potential for X-ray imaging detector s[8,9], and nuclear detectors for-rays and –particle s[10].

Several methods have been used for growing of mercuric iodide ploy-film such as laser ablation, growth from the vapor phase, screen print [11,12], electrodeposition, casting technique [13], and growth from solution[14]. Because of the high vapor pressure of HgI_2 below their melting point, the physical vapor deposition (PVD) was mainly adopted for the growth of large area mercuric iodide films. The film was successfully grown with area from tens to hundreds cm^2 [15,16], and thickness from tens to 1800μm [8,14,17,18]. The morphology of the films was also investigated for the needs of digital radiography [18]. Schieber thought that oriented growth was preferred to meet the need maximum radiation absorption [19]. Hence, the oriented poly-films matched with readout matrix pixellation are suitable for digital imaging.

Aim to dental X-ray unit, growth of large area mercuric iodide polycrystalline film (36cm^2) on Thin Film Transistor (TFT) with 256×256 pixels was investigated in present work. A polycrystalline film(1cm^2) on ITO was deposited by PVD in self-designed crystal growth furnace in previous study. XRD, SEM and *J-V* analysis were used to characterize the properties of these as-grown films. According to the test and analysis, the growth techniques of film were optimized. Large area HgI_2 polycrystalline films were grown using the same furnace.The texture of HgI_2 with 36cm^2 was analyzed by XRD. The direct image detector was then fabricated by using the 36cm^2 HgI_2 films.

2. Experimental procedure

High purity raw material of HgI_2 was acquired by the vapor phase synthesis at 200℃ using high pure Hg (7N) and I_2(5N). Material synthesized were vacuum sublimed for 4-6 times, followed by melting in rotated furnace at 300℃ for 3h. The ampoule for purification was carefully rinsed with acetone and de-ionized water, respectively. The repeated sublimation technique was employed to reduce impurities. Purified HgI_2 raw materials were introduced into the rinsed ampoule for film growth using the PVD. The whole growth cavity in furnace was sealed below a vacuum of 6.6×10^{-3}Pa. The temperature of deposition zone and source zone were set at 50 and 100℃, respectively, with the 4h of growth periodicity.

The texture of poly-film was studied by SHIMADZU 6000 X-ray diffraction with the X-ray wavelength of 1.5369Å. The surface morphology of the films was examined using a FEI Quanta 400FScanning Electron Microscope. *J-V* characteristic of as-grown film was measured by an Agilent 4155CVIV instrument at room temperature. The digital x-ray imaging was obtained by Nuctech Company Limited.

3. Results and discussion

Fig. 1 gives the SEM photography of as-grown HgI_2 film with the area of $1cm^2$. The grains of film are distinct crystalline borders with rectangular facets, and crystallite sizes are ranging from 100 to 150μm. XRD characteristic of films are given in Fig.2. According to the expressions $\sum I(00l)/\sum I(hkl)$, the orientation along [001] was evaluated to be approximately 94%, which indicated a relatively high texture. The electric transport properties of the poly-film were texted by Agilent 4155C instrument in the darkness, by attaching colloidal graphite with $0.1cm^2$ in area on the surface of as-grown HgI_2 film as top electrode, and ITO substrate as back one. Under a bias voltage between -100 V and 100V, the *J-V* curve of as-grown poly-HgI_2 film shows a good linearity, as shown in Fig.3.

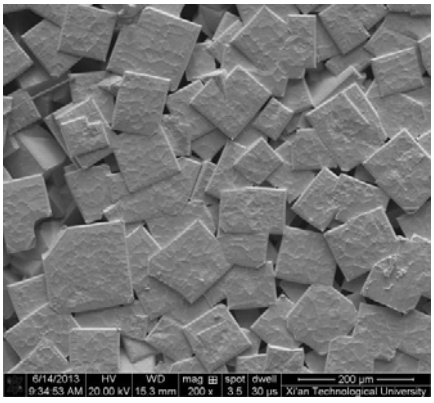

Fig. 1. SEM image of polyscrystalline HgI_2 film.

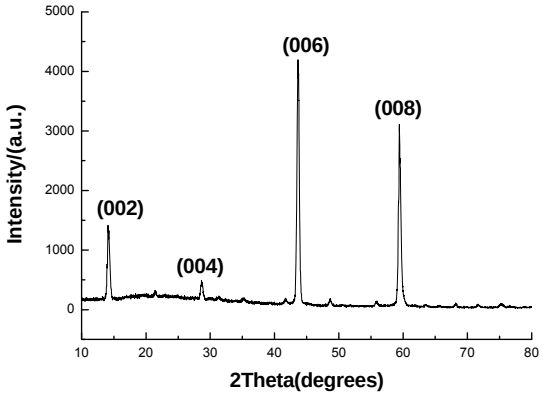

Fig. 2. XRD pattern of polyscrystalline HgI_2 film.

In Fig.3, the dark current density is amount to be the order of nA, with resistivity of approximately $2.2\times10^{11}\Omega\cdot$cm. Burger reported that the resistivity in the order of $10^{10}\Omega\cdot$cm for HgI_2 crystal was considered adequate to apply to detector [5]. Obviously, the electronic character of film could be satisfied with the need of X-ray and imaging detectors.

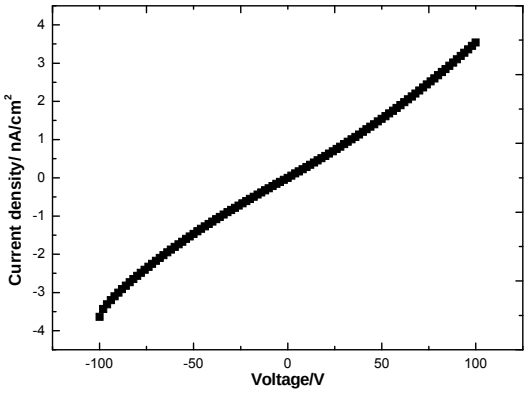

Fig. 3. J-V characteristic of polycrystalline HgI_2 film with colloidal graphite electrode.

However, there is much tint streaking on surface of grains, as shown in Fig.1. We deduced that it might be derived from volatilization of HgI_2 molecule on grain surface. Due to low thermal conductivity(4 and 20 mW/cm·K for the crystal directions parallel and perpendicular to the *c*-axis of HgI_2[20]), the temperature on growth interface was increasing with time. After 4h growth, temperature on back of ITO substrate was up to 57.3°C. Hence, high temperature at the growth surface of film lead to the volatilization of HgI_2 molecule and created

the tint marking on the facet of grains. Also, it can be seen in Fig.1 that grain size is about 120-150 μm, which is bigger than published work [1,7,21]. Numerous authors have reported that grain size was increased by higher substrate temperatures during deposition [22-24] .The higher the depositing temperature, the bigger grains sizes, the better the orientation of grains is. However, because of grain size matching readout pixel[18], it may be not very propitious to high resolution of digital imaging. Therefore, undesirable phenomena above may derive from longer growth time and higher temperature during deposition in all probability. Growth processing would be then adjusted.

Liquid crystal TFT with the area of 36cm^2, supplied by researchers affiliated with Nuctech Company Limited, was rinsed only in 18 MΩ de-ionized H_2O. Growth periodicity was set to be 2h for appropriate grains size. The back of TFT was also adhered carefully to the hydrocooling plane in growth furnace for faster cooling rate. The temperature of deposition zone decreased to 40□, and that of source kept to 100□.

Fig. 4. Mercuric iodide poly-film in 36cm^{2}area.

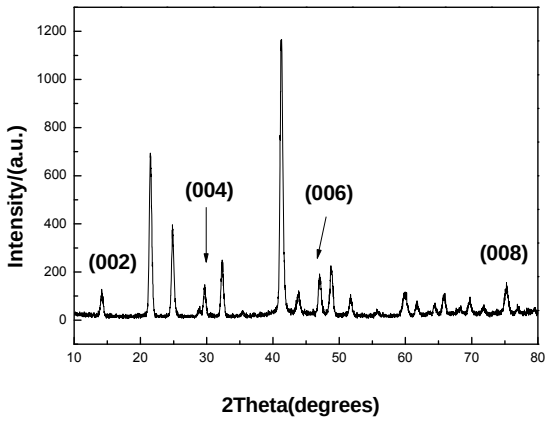

Fig. 5. XRD pattern of in polys-HgI_2 film.

Fig. 4 shows the result of mercuric iodide poly-film with 36cm^2 area grown in 2h periodic. It's obviously that red film distribute homogenously on TFT. In Fig. 5, besides of tiny {001} peak, many undesirable peaks were presented, which indicated a characteristic more close to basic stacking of HgI_2 powder. Schieber[19]thought that the kind of XRD pattern of HgI_2 film was not good for maximum radiation absorption because of bad preferred orientation. Clearly, inadequate growth occurs due to lower temperature of deposition.

The thickness of larger area film has thinner than that of one with 1cm^2 in areas. So graphite adhesive tape was adhered onto the top electrode replacing colloidal graphite, prohibiting colloidal permeate to the bottom of film. The graphite adhesive tape was adhered the surface of as-grown HgI_2 film as much as possible. The capsulation and image-acquired system were carried by Nuctech Company Limited. X-ray image was obtained under 80keV with 6mA current.

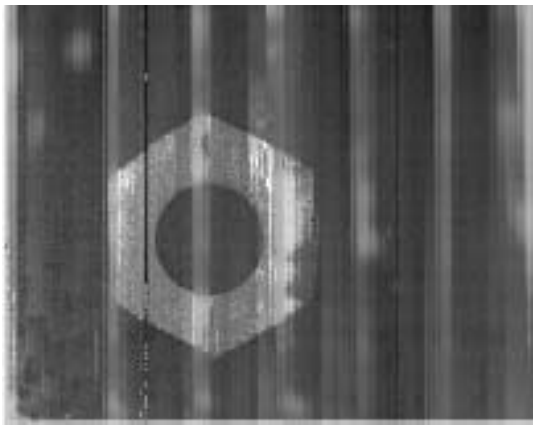

Fig. 6. Nut image taken by X-ray Planar Images.

Fig. 6 shows planar X-ray image on a 256×256 pixel HgI_2-coated array. The outer hexagon and the inner circular shape of the non-corrosive steel nut with Φ 6mm are distinctly appeared. The upper layer of the top electrode was graphite adhesive tape, which was adhered on the surface of HgI_2 film by hand. Untight electrode attachment between graphite adhesive tape and film may lead to the distortion of imaging at the lower right of the nut.

According to XRD pattern in Fig.5, thin film consists of powder grain. Too much grain boundary reduces the charge transport efficiency due to their recombination/electrical barriers. However, compact accumulation of grains reduces charge shunting via pinholes and leakage path, increases the response to X-ray. Hence, the adjustment of growth craft in this processing may be suitable for matrix preservation.

Obviously, present result is rather satisfied with dental X-ray unit. Firstly, the better the orientation, the better the charge transport along *c*-axis of microcrystals [1,25] . Although the image of nut is presented, it has the probability to further improve the imaging effect because the resistivity of oriented films is the 2 order of higher than that one of poly-films [1]. Secondly, thinner thickness of films must be the challenging of electrode preparing, whatever by sputtering and evaporation of Au/Pd because of high vapor of mercuric iodide, or coating colloidal graphite due to the possibility of permeating to the bottom of film. What's more, graphite adhesive tape commonly used in SEM could not acquire tight contact on film by hand. Accordingly, future effort may attribute to optimize the growth processing for thick films of HgI_2.

4. Conclusions

The paper presents direct conversion X-ray images obtained with HgI_2 poly-film. Different areas of HgI_2 poly-film have been grown by PVD using self-design crystal growth furnace. Film with $1cm^2$ in area was investigated by XRD and SEM. The results show that the ratio of (*001*) / (*hkl*) on as-grown films is amount to be 94%. From *J-E* measurements, the value of ρ in $1cm^2$ film approaches to about10^{11} Ω·cm, indicating reasonable purification processing of raw material. The large area poly-film ($36cm^2$) was successfully grown on TFT through optimization of growth craft. The XRD measurement shows that texture of as-grown films is close to that of HgI_2 powder. Imaging of the nut displays clear outline. We believe that compact accumulation of grains increases the compactness of films, reduces carrier shunting via pinholes and leakage path, and then increases the response to X-ray.

Acknowledgments

We are grateful to the National Natural Science Foundation of China (No.51502234) , the Open Fund of the Shaanxi Key Laboratory of Optoelectronic Functional Materials and Devices (No. ZSKJ201414), and the Scientific research plan projects of Shaanxi provincial department of Education (No. 15JS040) for providing us with financial support in the form of a research project.

Reference

[1] L. Fornaro, I. Aguiar, A. Noguera, M. Pérez, IEEE Nuclear Science Symposium Conference Record **2**, 878 (2005).

[2] M. Pérez, I. Noguerol, L. Fornaro, Nucl.Instrum. Methods. Phys. Res A **610**, 328 (2009).

[3] W. C. Barber, N. E. Hartsough, J.S. Iwanczyk, IEEE Trans.Nucl.Sci. NS-56, 1012 (2009).

[4] A.Burger, D. Nason, L. Franks, J. Cryst.Growth **379**, 3 (2013).

[5] W. C. Barber, N.E. Hartsough, M.Q. Damron, J.S. Iwanczyk, IEEE Nuclear Science Symposium Conference Record N06-5, 78 (2007).

[6] N. E. Hartsough, J. S. Iwanczyk, B. E. Patt, N. L.Skinner, IEEE Trans.Nucl.Sci. **51**, 1812 (2004).

[7] J. S. Iwanczyk, E. P. Bradley, C. R. Tull, L. R. Macdonald, N. Skinner, E. J. Moffman, L.Fornaro, L. Mussio, E. Saucedo, A. Gancharov Proc. SPIE **4508**, 119 (2001).

[8] M. Schieber , H. Hermon, A. Zuck, A. Vilensky, L. Melekhov, R. Shatunovsky, E. Meerson, Y. Saado, M. Lukach, E. Pinkhasyc, S. E. Ready, R. A. Street, J. Cryst.Growth, **225**, 118 (2001).

[9] R. Turchetta , W. Dulinski, D. Husson, J. L. Riester, M. Schieber, A. Zuck, L. Melekhov, Y. Saado, H. Hermon, J. Nissenbaum, Nucl.Instrum. Methods. Phys. Res A **428**, 88 (1999)

[10] M. Schieber, A. Zuck, M. Braiman, J. Nissenbamn, R. Turchetta, W. Dulinski, D. Husson, J. L. Riester, Nuclear Physics B, **61**, 321 (1998).

[11] M. Schieber, H.Hermon, A.Zuck, A.I.Vilensky, L.Melekhov, R.Shatunovksy, E.Meerson,Y.Saaso, Proc. SPIE **3115**, 146 (1999).

[12] M. M. Schieber, A. Zuck, L. Melekhov, R. Shatunovksy, H. Hermon, R.A.D. Turchetta, Proc. SPIE **3768**, 296 (1999).

[13] J. C. Ugucioni, T. G. Netto, M. Mulato, Nucl.Instrum. Methods. Phys. Res A. **622**, 157 (2010).

[14] J. S. Iwanczyk, B. E. Patt, C. R. Tull, L. R. MacDonald, N. Skinner, L. Fornaro, IEEE Trans.Nucl.Sci. **49**, 160 (2002).

[15] G. Xu, Y. F. Guo, Z. Z Xi, Z. Gu, L. Zhang, W. T. Yu, X. M. Ma, B. Li, Proc. SPIE **9298**, 91 (2014).

[16] N. E. Hartsough, J. S. Iwanczyk, E. Nygard, N. Malakhov, W. C. Barber, T. Gandhi. IEEE Nuclear Science Symposium Conference Record, **R12-78**, 370 (2008).

[17] U. N. Roy, Y. Cui, G. Wright, C. Barnett, A. Burger, L. A. Franks, Z. W. Bell, IEEE Trans.Nucl.Sci. **49**, 1965 (2002).

[18] L. Fornaro, J. Cryst.Growth, **371**, 155 (2013).

[19] M. Schieber, A. Zuck, J. Optoelectron. Adv. M. **5**, 1299 (2003).

[20] M. Isshiki, M. Piechotka, E. Kaldis, J. Cryst.Growth, **102**, 344 (1990)
[21] M. Schieber, A. Zuck, H. Gilboa, G. Zentai, IEEE Trans.Nucl.Sci. **53**, 2385 (2006).
[22] J. Luschitz, K. Lakus-Wollny, A. Klein, W. Jaegermann, Thin Solid Films, **515**, 5814 (2007).
[23] J. Luschitz, B. Siepchen, J. Schaffner, K. Lakus-Wollny, G. Haindl, A. Klein, W. Jaegermann, Thin Solid Films, **517**, 2125 (2009).
[24] C. S. Ferekides, D. Marinskiy, S. Marinskaya, B. Tetali, IEEE Photovoltaic Specialists Conference, 751 (1996).
[25] W. G. Yang, L. Nie, D. M. Li, Y. L. Wang, J. Zhou, L. Ma, Z. H. Wang, W. M. Shi, J. Cryst.Growth, **324**,149 (2011).

*Corresponding author:xxrshhuangshan@126.com